JOURNAL OF GUIDANCE, CONTROL, AND DYNAMICS
Vol. 19, No. 5, September–October 1996

Robust Control of Passive-Jointed Robot and Experimental Validation Using Sliding Mode

Paul I. Ro and Chih-Chen Yih
North Carolina State University, Raleigh, North Carolina 27695-7910

A robust control strategy for a passive-jointed robot using sliding mode control is investigated. Instead of an actuator, the passive joint has a brake to reduce the weight and energy consumption of the robot. While the brake is released, the passive joint is indirectly controlled by the motion of the active joint using the dynamic coupling of the robot manipulators. However, there are uncertainties associated with parameters in the links as well as in the operation of the actuator and the brake. To ensure minimum variation from the desired mode of operation in the presence of these uncertainties, a sliding mode control algorithm is developed and the performance evaluated. From simulation results, the sliding mode scheme is superior to a simple computed torque method in terms of passive-joint tracking performance and robustness. A two-link manipulator was designed and built to evaluate the proposed control scheme experimentally. The robot consists of one active joint and one passive joint and operates in a horizontal plane. The planar manipulator was controlled from a 32-bit 80486 microcomputer via DT2811 input/output board. The experimental results indicate that the sliding mode controller, when compared to the computed torque controller, reduces the tracking error by 50% and improves the robustness to variations in payloads.

Nomenclature

$b_{\max}$, $f_{\max}$	= maximum of b, f
$b_{\min}$, $f_{\min}$	= minimum of b, f
$\hat{b}$, $\hat{f}$, $\hat{u}$	= estimate of b, f, u
C	= nonlinear Coriolis, centripetal terms, and gravitational forces
F, β	= bound on uncertainties
H	= inertial matrix
k	= switching gain
n	= degree of freedom
$\boldsymbol{q}$	= vector of $n-r$ passive joints and the vector of $2r-n$ active joints
$\boldsymbol{q}_d$	= desired value of q
r	= number of active joints
$\boldsymbol{s}$	= sliding surface
t	= time
$\boldsymbol{u}$	= control input
$\|x\|$	= norm of x
z	= vector of $n-r$ active joints
Δb	= difference between b and $\hat{b}$
Δf	= difference between f and $\hat{f}$
η	= positive real number
$\boldsymbol{\theta}$	= vector of generalized coordinates
λ	= positive constant
τ	= vector of generalized force
Υ_1, Υ_2	= positive real number
Φ	= thickness of the boundary layer

I. Introduction

IN space, the cost of fuel is the one overriding factor in determining the nature of automation. Recently, much work has been done to address various issues concerning robotization of some maintenance, repair, and construction tasks in space. Teleoperation with

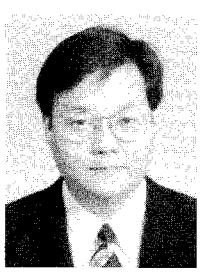

Paul I. Ro received his B.S. from the University of Minnesota and M.S. and Ph.D. degrees from the Massachusetts Institute of Technology, all in Mechanical Engineering, in 1982, 1985, and 1989, respectively. He became Assistant Professor in the Mechanical and Aerospace Engineering Department, North Carolina State University, in 1989, and was promoted to Associate Professor in 1994. In 1995, he was a Visiting Associate Professor at the Department of Machine Design and Production Engineering, Seoul National University, Seoul, Republic of Korea. His fields of research are precision mechatronics and control, microdynamics of mechanical slides, ultra-high precision machining, magnetic servo levitation, nonholonomic motion planning and control, robotic assembly, and intelligent vehicle control. He is a member of the American Society of Mechanical Engineers and American Society of Precision Engineers (ASPE) and is an Associate Editor of *Precision Engineering*, the journal of ASPE.

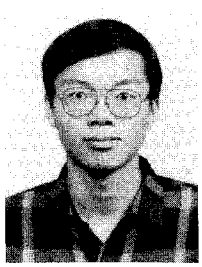

Chih-Chen Yih received his B.S. in Mechanical Engineering from National Cheng Kung University, Taiwan, in 1990. He has worked for Philips Taiwan Company as an automation engineer since 1992. Currently, he is a Ph.D. student under Paul I. Ro in the Department of Mechanical Engineering, North Carolina State University. His research interests are nonlinear control of mechanical systems and intelligent control.

Received Jan. 18, 1995; revision received April 25, 1996; accepted for publication May 3, 1996.

remote sensing, two-arm coordination, free-floating robot manipulator, and passive-jointed robot manipulator have resulted from an ongoing search for the best man–machine combination system for space operations that can be realized with a minimum cost. Passive-jointed robots can be an ideal choice for space operation because, in general, they require less power and less instrumentation, and weigh less. With fewer actuators, the passive-jointed robot will be easier to design and provide low-cost automation. The main idea behind the design of passive-jointed robot manipulators is the coupling of dynamics between joints that are controlled actively and the joints that have passive connections. The coupled dynamics can be utilized to control the angles of passive joints indirectly by controlling the active joints.

The position control of a manipulator composed of active and passive joints was discussed in Ref. 1. The passive joints were assumed to have brakes instead of actuators. When the brakes were engaged, the passive joints were fixed and the active joints were controlled. When the brakes were released, the passive joints were indirectly controlled by the coupling characteristics of the manipulator dynamics. The position of the manipulator was controlled by engaging and releasing the brakes. A basic controllability of such a system using a linearized dynamics has been shown in Ref. 1. Also, the same work proposed a simple control scheme based on the computed torque method and demonstrated the cost saving feasibility of such approach. The work[1] opened new design and control possibilities for space robots in general. However, control in the presence of uncertainties and unmodeled dynamics have not been addressed. Because full trajectory control is not possible for an obvious reason, it becomes very crucial to address the robustness characteristics of the passive-jointed robot. The control scheme for passive-jointed robot can also be applied to the completely actuated manipulators with failed joints.[2,3] We can utilize the dynamic coupling between the failed and working joints to control the failed joints to their values and lock them by using brakes.

To ensure minimum variation from the desired mode of operation of the actuator and the brake in the presence of system uncertainties and environmental disturbances, a sliding mode control scheme using variable structure system theory[4–9] is applied to the passive-jointed robot. The sliding mode controller is designed in such a way that all state trajectories are directed toward the sliding surface. Once the system state reaches the sliding surface, it slides along the surface and the system response depends only on the equations that define the surface and thus remains robust to the disturbance and parameter variations.[10–13]

Simulation results show that the sliding mode scheme is superior to the computed torque method in dealing with parametric uncertainties. A two-link experimental robot was designed and built to study the feasibility of the passive-jointed robot. The sliding mode control algorithm was also implemented on a microcomputer. The performance of the sliding mode control is validated by experimental results performed on the two-link passive-jointed robot.

This paper is organized as follows. Section II begins the discussion of the dynamic equation of the passive-jointed robot. Section III generalizes the sliding mode control to the multi-input nonlinear system and then is applied to our passive-jointed robot. Based on the Lyapunov stability criterion, the switching gain is derived to track the trajectory of the passive joint of the robot. Section IV applies our proposed sliding mode controller to a two-link planar passive-joint robot. Section V discusses the results of the experimental implementation of the sliding mode controller. Section VI presents some conclusions.

II. Dynamic Model

In this paper we consider a manipulator with n degrees of freedom. We assume that r [$r \geq (n/2)$] degrees of freedom of the manipulator are active joints with actuators and $n - r$ degrees of freedom are passive joints with brakes instead of actuators. When the brakes are locked, the active joints can be controlled without affecting the state of the passive joint. When the brakes are released, the passive joints are free and indirectly controlled by the coupling forces generated by the motion of active joints. Assuming the joints are frictionless and contain no other disturbances, the dynamic equations of an n-link rigid manipulator can be written as[14]

$$H(\theta)\ddot{\theta} + C(\theta, \dot{\theta}) = \tau \tag{1}$$

where θ is the vector of the joint displacements; $H(\theta)$ is an inertia matrix; $C(\theta, \dot{\theta})$ is a matrix that contains the nonlinear Coriolis, centripetal terms, and gravitational forces; and τ is the joint torque vector.

It is assumed that z is a vector of $n - r$ active joint positions; q is a vector of $n - r$ passive joint positions and $2r - n$ active joint positions.[1] When $r = n/2$, q is a vector of $n/2$ passive joint positions.

We can rearrange θ as

$$\theta = \begin{bmatrix} z \\ q \end{bmatrix} \begin{matrix} n-r \\ r \end{matrix} = \begin{bmatrix} z \\ q_{\text{act}} \\ q_{\text{pas}} \end{bmatrix} \begin{matrix} n-r \\ 2r-n \\ n-r \end{matrix} \tag{2}$$

The $n - r$ passive joints q_{pas} are controlled through dynamic coupling by the motion of the $n - r$ active joints z. Position control of passive-jointed robot can be done in two steps. First, the $n - r$ passive joints q_{pas} are controlled indirectly by $n - r$ active joints z. Second, after the passive joints q_{pas} are locked by brakes at the desired positions, the $n - r$ active joints z and $2r - n$ active joints q_{act} are then controlled by actuators. Therefore, both passive joints and active joints can be controlled to their desired positions by using brakes and actuators.

To express the dynamic equations such that the passive joints can be controlled directly by the active joints, one can now partition $H(\theta)$, $C(\theta, \dot{\theta})$, τ as follows[1]:

$$H(\theta) = \begin{bmatrix} H_{11}(\theta) & H_{12}(\theta) \\ H_{21}(\theta) & H_{22}(\theta) \end{bmatrix} \begin{matrix} r \\ n-r \end{matrix} \tag{3}$$

$$\begin{matrix} n-r & r \end{matrix}$$

$$C(\theta, \dot{\theta}) = \begin{bmatrix} C_1(\theta, \dot{\theta}) \\ C_2(\theta, \dot{\theta}) \end{bmatrix} \begin{matrix} r \\ n-r \end{matrix} \tag{4}$$

$$\tau = \begin{bmatrix} \tau_1 \\ \tau_2 \end{bmatrix} \begin{matrix} r \\ n-r \end{matrix} \tag{5}$$

When the passive joints are free, the joint torque of the passive joints are equal to zero; then $\tau_2 = 0$.

Substituting Eqs. (2–5) into Eq. (1) we obtain

$$H_{11}\ddot{z} + H_{12}\ddot{q} + C_1 = \tau_1 \tag{6}$$

$$H_{21}\ddot{z} + H_{22}\ddot{q} + C_2 = \mathbf{0} \tag{7}$$

If H_{21} is not singular, Eq. (7) can be solved for $\ddot{z}$ to yield

$$\ddot{z} = -H_{21}^{-1}H_{22}\ddot{q} - H_{21}^{-1}C_2 \tag{8}$$

Equation (8) is used to eliminate $\ddot{z}$ in the Eq. (6) as

$$\tilde{H}\ddot{q} + \tilde{C} = \tilde{\tau} \tag{9}$$

where

$$\tilde{H} = H_{12} - H_{11}H_{21}^{-1}H_{22}, \qquad \tilde{C} = C_1 - H_{11}H_{21}^{-1}C_2, \qquad \tilde{\tau} = \tau_1$$

The matrix H_{21} corresponds to the dynamic coupling between the active joints and the passive joints, and it depends on the structure and mass distribution of the manipulator.[15] As shown in Ref. 1, the condition of output controllability is equivalent to the condition necessary to solve the generalized for the active joint (i.e., H_{21} is not singular). Since H_{21} is related to the mechanical structure of the manipulators, one should keep H_{21} away from its singular points when considering the robot arm design.

The dynamic equations can be further reduced as

$$\ddot{q} = f(q) + b(q)u \tag{10}$$

where

$$\boldsymbol{q} = \begin{bmatrix} \boldsymbol{q} \\ \dot{\boldsymbol{q}} \end{bmatrix}, \qquad f(\boldsymbol{q}) = -\tilde{H}^{-1}\tilde{C}, \qquad b(\boldsymbol{q}) = \tilde{H}^{-1}, \qquad \boldsymbol{u} = \tilde{\boldsymbol{\tau}}$$

Equation (10) represents a nonlinear and time-varying dynamic model. The control problem is to get the state $\boldsymbol{q}$ to track a specific time varying $\boldsymbol{q}_d$ in the presence of model imprecision on $f(\boldsymbol{q})$ and $b(\boldsymbol{q})$.

III. Sliding Mode Control

We now have to design a control law that utilizes the coupling dynamics to control the passive joints and reject the system uncertainty resulting from parametric variation and disturbance. Based on variable structure system theory, a sliding mode control scheme is considered to control the trajectories of the passive joints in the presence of modeling imprecisions.

Sliding mode control consists of two steps. In the first, the control law forces the trajectory toward the sliding surface, whereas in the second step, the controller is smoothed inside a boundary layer.[16] We now assume that there are parametric variations and disturbance for our model. The dynamic equation can be written as

$$\ddot{\boldsymbol{q}} = f(\boldsymbol{q}) + b(\boldsymbol{q})\boldsymbol{u} \tag{11}$$

A nominal model for sliding mode control is given as

$$\ddot{\boldsymbol{q}} = \hat{f}(\boldsymbol{q}) + \hat{b}(\boldsymbol{q})\hat{\boldsymbol{u}} \tag{12}$$

Assuming some bounds on uncertainties on $f(\boldsymbol{q})$ and $b(\boldsymbol{q})$ to be

$$\|\Delta f\| \le \Upsilon_1 \tag{13}$$

$$\|\Delta b\| \le \Upsilon_2 \tag{14}$$

the norm of a matrix A is defined as

$$\|A\| = \sup_{x \neq 0} \frac{\|Ax\|}{\|x\|} = \sup_{\|x\|=1} \|Ax\|$$

The uncertainties Δf in Eq. (13) and Δb in Eq. (14) are defined as

$$\Delta f = f - \hat{f} \tag{15}$$

$$\Delta b = b - \hat{b} \tag{16}$$

where

$$\hat{f} = \frac{f_{\max} + f_{\min}}{2} \tag{17}$$

$$\hat{b} = \frac{b_{\max} + b_{\min}}{2} \tag{18}$$

We then define

$$\Upsilon_1 = \left\| \frac{f_{\max} - f_{\min}}{2} \right\| \tag{19}$$

$$\Upsilon_2 = \left\| \frac{b_{\max} - b_{\min}}{2} \right\| \tag{20}$$

Note that Υ_1 and Υ_2 are nonnegative real numbers.

First, we choose a sliding surface $\boldsymbol{s}$ as a function of the output trajectory error

$$\boldsymbol{s} = \dot{\tilde{\boldsymbol{q}}} + \Lambda\tilde{\boldsymbol{q}} = \boldsymbol{0} \tag{21}$$

where $\tilde{\boldsymbol{q}} = \boldsymbol{q} - \boldsymbol{q}_d$, $\dot{\tilde{\boldsymbol{q}}} = \dot{\boldsymbol{q}} - \dot{\boldsymbol{q}}_d$ and $\Lambda = \text{diag}[\lambda_1\ \lambda_2\ \cdots\ \lambda_n]$, $\lambda_i > 0$, $i = 1, 2, \ldots, n$. The positive gains λ_i determine the rate of response of the system. Then, we derive a control law to drive the system to the sliding surface. The Lyapunov stability criterion is used to derive a sliding condition such that the sliding surface can be reached within a finite time. We choose a Lyapunov function $v = \frac{1}{2}\boldsymbol{s}^T \cdot \boldsymbol{s}$. By applying the Lyapunov stability criterion $\dot{v} \le 0$, a sliding condition is obtained as

$$\dot{v} = \boldsymbol{s}^T \cdot \dot{\boldsymbol{s}} \le 0 \tag{22}$$

To make sure $\dot{v}(\boldsymbol{s}, \dot{\boldsymbol{s}})$ vanishes only at $\boldsymbol{s} = \boldsymbol{0}$, the preceding equation can be modified as

$$\dot{v} = \boldsymbol{s}^T \cdot \dot{\boldsymbol{s}} \le -\eta\|\boldsymbol{s}\| \tag{23}$$

where η is a positive real number to adjust the approaching speed toward the sliding surface.

The sliding condition can be expressed as

$$\frac{1}{2}\frac{\mathrm{d}}{\mathrm{d}t}(\boldsymbol{s}^T \cdot \boldsymbol{s}) \le -\eta\|\boldsymbol{s}\| \tag{24}$$

Once the trajectory is on the surface (in the sliding mode), the dynamics can be written as $\dot{\boldsymbol{s}} = 0$.

For the nominal model, we obtain

$$\dot{\boldsymbol{s}} = \hat{f} + \hat{b}\hat{\boldsymbol{u}} - \ddot{\boldsymbol{q}}_d + \Lambda\dot{\tilde{\boldsymbol{q}}} = \boldsymbol{0} \tag{25}$$

Solve this equation for the control input to get the equivalent control

$$\hat{\boldsymbol{u}} = \hat{b}^{-1}(-\hat{f} + \ddot{\boldsymbol{q}}_d - \Lambda\dot{\tilde{\boldsymbol{q}}}) \tag{26}$$

However, to account for the presence of modeling imprecision and of disturbance, we add to $\hat{u}$ a term discontinuous across the surface $\boldsymbol{s} = 0$,

$$\boldsymbol{u} = \hat{\boldsymbol{u}} - \hat{b}^{-1}k \cdot \text{sgn}(\boldsymbol{s}) \tag{27}$$

where

$$\text{sgn}(s_i) = \begin{cases} 1 & s_i > 0 \\ 0 & s_i = 0 \\ -1 & s_i < 0 \end{cases} \tag{28}$$

and k is the switching gain.

In fact, one can think of the sliding mode controller as consisting of two parts. Here, $\hat{\boldsymbol{u}}$ is the control for the nominal model and $-\hat{b}^{-1}k \cdot \text{sgn}(\boldsymbol{s})$ is dealing with uncertainties. This switching gain k will keep the state trajectory on the sliding surface; thus the system is robust to parameters uncertainties. The selection of the gain k should be made to guarantee the stability of the s dynamics as follows:

$$\dot{\boldsymbol{s}} = (f - \hat{f}) + (b\,\hat{b}^{-1} - I)(-\hat{f} + \ddot{\boldsymbol{q}}_d - \Lambda\dot{\tilde{\boldsymbol{q}}}) - b\,\hat{b}^{-1}k \cdot \text{sgn}(\boldsymbol{s}) \tag{29}$$

Substituting Eq. (29) into Eq. (23) and applying the uncertainties defined in Eqs. (15) and (16), we obtain

$$\boldsymbol{s}^T \cdot \left[\Delta f + \Delta b\,\hat{b}^{-1}(-\hat{f} + \ddot{\boldsymbol{q}}_d - \Lambda\dot{\tilde{\boldsymbol{q}}}) - (I + \Delta b\,\hat{b}^{-1})k \cdot \text{sgn}(\boldsymbol{s})\right] \le -\eta\|\boldsymbol{s}\| \tag{30}$$

We can use the following inequalities to simplify Eq. (30):

$$-\boldsymbol{s}^T \cdot \Delta b\,\hat{b}^{-1}k \cdot \text{sgn}(\boldsymbol{s}) \le k\|\boldsymbol{s}\|\,\|\Delta b\|\,\|\hat{b}^{-1}\text{sgn}(\boldsymbol{s})\| \tag{31}$$

$$-\boldsymbol{s}^T \cdot k \cdot \text{sgn}(\boldsymbol{s}) \le k\|\boldsymbol{s}\| \tag{32}$$

By applying the preceding inequalities, Eq. (30) becomes

$$\|\boldsymbol{s}\| \cdot \left[\Upsilon_1 + \Upsilon_2\left\|\hat{b}^{-1}(-\hat{f} + \ddot{\boldsymbol{q}}_d - \Lambda\dot{\tilde{\boldsymbol{q}}})\right\| - k\left(1 - \Upsilon_2\|\hat{b}^{-1}\text{sgn}(\boldsymbol{s})\|\right)\right] \le -\eta\|\boldsymbol{s}\| \tag{33}$$

The gain k is found as

$$k \ge \frac{\Upsilon_1 + \Upsilon_2\left\|\hat{b}^{-1}(-\hat{f} + \ddot{\boldsymbol{q}}_d - \Lambda\dot{\tilde{\boldsymbol{q}}})\right\| + \eta}{1 - \Upsilon_2\|\hat{b}^{-1}\text{sgn}(\boldsymbol{s})\|} \tag{34}$$

The control law $\boldsymbol{u}$ is discontinuous across the switching surface $\boldsymbol{s} = 0$. Since the switching is not instantaneous in practice, the imperfection in the switching leads to undesirable chattering. This adverse

Table 1 System parameters

m_1, kg	m_2, kg	m_3, kg	I_1, kgm^2	I_2, kgm^2	l_1, m	l_{1c}, m	l_2, m	l_{2c}, m
0.874	0.836	2.857	0.1148	0.0065	0.397	0.1985	0.305	0.1525

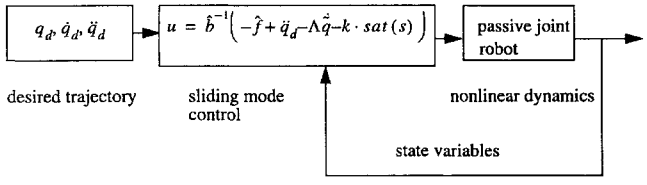

Fig. 1 Sliding mode control scheme.

chattering effect may excite high-frequency dynamics neglected in the modeling and require greater control effort. To avoid exciting high-frequency unmodeled dynamics, one can use the boundary-layer function to smooth the discontinuous slide mode control and to achieve robustness.[13] The sgn(s) function is replaced by the sat(s) function defined as

$$\text{sat}(s_i) = \begin{cases} 1 & s_i > \Phi \\ s_i/\Phi & |s_i| \le \Phi \\ -1 & s_i < -\Phi \end{cases} \tag{35}$$

The boundary layer will lead to tracking within a guaranteed precision instead of perfect tracking. The smoothing of control discontinuity inside the boundary Φ essentially serves as a low-pass filter to the variable s near the sliding surface, thus eliminating chattering.[12] Therefore, the sliding mode control law is given by

$$\boldsymbol{u} = \hat{\boldsymbol{u}} - \hat{b}^{-1}k \cdot \text{sat}(s) = \hat{b}^{-1}[-\hat{f} + \ddot{q}_d - \Lambda\dot{\tilde{q}} - k \cdot \text{sat}(s)] \tag{36}$$

The sliding mode control scheme for the passive-jointed robot is shown in Fig. 1.

IV. Simulation Results

Here the sliding mode control algorithm is applied to the two-link passive-jointed robot, shown in Fig. 2, whose parameters are given in Table 1. The two-link robot has one active joint equipped with a motor for providing control torque and one passive joint equipped with a brake. The brake is modeled as one mass at the passive joint. The dynamic equation is given by

$$\begin{bmatrix} H_{11} & H_{12} \\ H_{21} & H_{22} \end{bmatrix} \begin{bmatrix} \ddot{z} \\ \ddot{q} \end{bmatrix} + \begin{bmatrix} C_1 \\ C_2 \end{bmatrix} = \begin{bmatrix} \tau_1 \\ 0 \end{bmatrix} \tag{37}$$

where

$$H_{11} = m_1 l_{c1}^2 + I_1 + m_2\left(l_1^2 + l_{c2}^2 + 2l_1 l_{c2}\cos q\right) + I_2 + m_3 l_1^2$$

$$H_{22} = m_2 l_{c2}^2 + I_2, \qquad H_{12} = H_{21} = m_2 l_1 l_{c2}\cos q + m_2 l_{c2}^2 + I_2$$

$$h = m_2 l_1 l_{c2}\sin q, \qquad C_1 = -2h\dot{z}\dot{q} - h\dot{q}^2, \qquad C_2 = h\dot{z}^2$$

If H_{21} is not singular, we can solve $\ddot{z}$ as

$$\ddot{z} = -(H_{22}/H_{21})\ddot{q} - (h/H_{21})\dot{z}^2 \tag{38}$$

The dynamic equations can be further reduced as

$$\ddot{q} = f(\boldsymbol{q}) + b(\boldsymbol{q})u \tag{39}$$

where

$$\boldsymbol{q} = \begin{bmatrix} q \\ \dot{q} \end{bmatrix}$$

$$f(\boldsymbol{q}) = \left[H_{12} - \left(\frac{H_{11}H_{22}}{H_{21}}\right)\right]^{-1}\left(\frac{H_{11}h}{H_{21}}\dot{z}^2 + 2h\dot{z}\dot{q} + h\dot{q}^2\right)$$

$$b(\boldsymbol{q}) = \left[H_{12} - \left(\frac{H_{11}H_{22}}{H_{21}}\right)\right]^{-1}, \qquad u = \tau_1$$

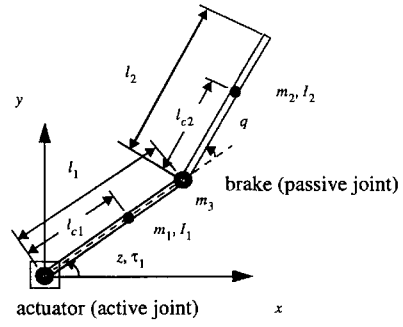

Fig. 2 Two-link planar passive-jointed robot.

We now assume that there are parametric inaccuracies for our model. The equation can be written as

$$\ddot{q} = f_u(q) + b_u(q)\tau_1 \tag{40}$$

To test the performance of the sliding mode controller, we assumes a uncertainty of ±50% on f and ±20% on b. In the simulation, we let

$$f_u(q) = (1 + 0.5\sin 6\pi t)f(q) \tag{41}$$

$$b_u(q) = (1 + 0.2\sin 6\pi t)b(q) \tag{42}$$

Therefore, the bounds on uncertainties on $f_u(q)$ and $b_u(q)$ are

$$|f_u - \hat{f}| \le \Upsilon_1 \tag{43}$$

$$|b_u - \hat{b}| \le \Upsilon_2 \tag{44}$$

where

$$\hat{f} = f, \qquad \hat{b} = b, \qquad \Upsilon_1 = 0.5|f|, \qquad \Upsilon_2 = 0.2|b|$$

The desired trajectory is

$$q_d = -(\pi/4)(1 - \cos \pi t) \tag{45}$$

For our two-link planar robot, the desired trajectory is assumed to be continuous. Therefore, the desired trajectory must start with the same position and velocity as those of the system. The initial conditions are in radians and radians per second

$$z = 0, \qquad \dot{z} = 0, \qquad q = 0, \qquad \dot{q} = 0$$

First, we choose a sliding surface s as a function of the output trajectory error

$$s = \dot{\tilde{q}} + \lambda\tilde{q} = 0 \tag{46}$$

where $\tilde{q} = q - q_d$ and $\dot{\tilde{q}} = \dot{q} - \dot{q}_d$.

The sat(s) function is defined as

$$\text{sat}(s) = \begin{cases} 1 & s > \Phi \\ s/\Phi & |s| \le \Phi \\ -1 & s < -\Phi \end{cases} \tag{47}$$

The control law is given by

$$u = \hat{u} - \hat{b}^{-1}k \cdot \text{sat}(s) = \hat{b}^{-1}[-\hat{f} + \ddot{q}_d - \lambda\dot{\tilde{q}} - k \cdot \text{sat}(s)] \tag{48}$$

where

$$k \ge \frac{\Upsilon_1 + \Upsilon_2\left|\hat{b}^{-1}(-\hat{f} + \ddot{q}_d - \lambda\dot{\tilde{q}})\right| + \eta}{1 - \Upsilon_2|\hat{b}^{-1}\text{sgn}(s)|} \tag{49}$$

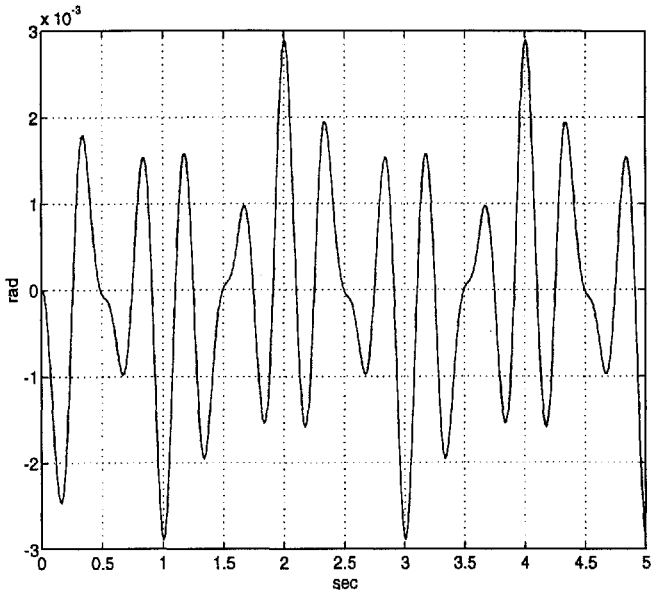

Fig. 3 Tracking error under sliding mode control.

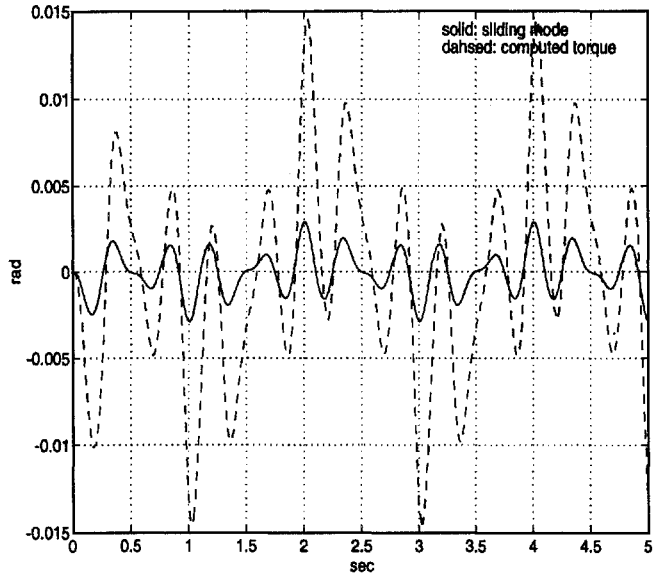

Fig. 4 Tracking error comparison.

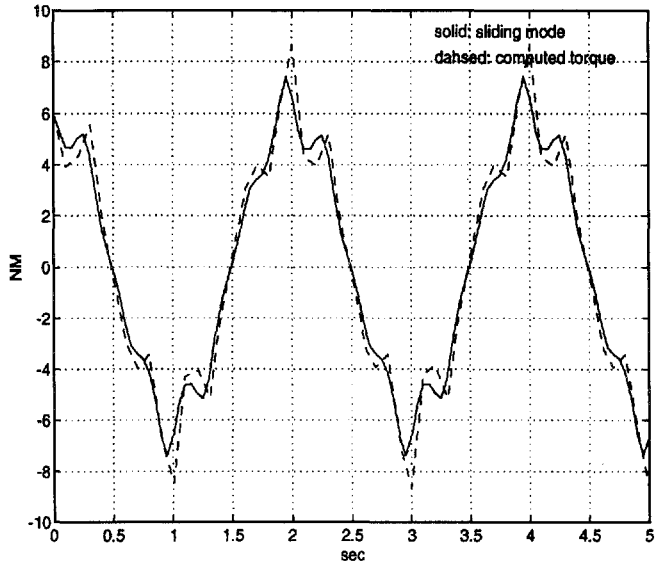

Fig. 5 Control torque comparison.

The value of λ was chosen to be 10, which was used to define the sliding surface in Eq. (46). To eliminate the unwanted chattering, Φ was selected as 2.0. The parameter η is chosen to be 40 for the state trajectories to reach the boundary layer fast. The tracking error of the robot under the sliding mode control is shown in Fig. 3. To compare with the sliding control in previous section, we use computed torque control. The same uncertainty is assumed with the same system. The corresponding tracking error and control torque are shown in Figs. 4 and 5.

As shown in Figs. 4 and 5, the tracking error is much smaller (50% less) under sliding control than under computed torque control. The sliding control also requires a smaller control torque to track the desired trajectory. The results clearly show that sliding control is an effective controller in the presence of model uncertainty.

V. Experimental Results

A. Experimental Robot

The planar manipulator hardware, computer, and interfacing are described in this section. The two-link passive-jointed robot shown in Fig. 6 was used to experimentally evaluate the proposed sliding mode control. It includes a robotic device with two revolute joints arranged so that the arm operates in a horizontal plane. The active joint (shoulder joint) is equipped with a dc motor with rated torque at 508 oz-in. that rotates the arm in the horizontal plane. The passive joint is the elbow joint, which is a free joint when the brake is released. Because the motion occurs only in the horizontal plane, we do not have to take into account the effect of gravity. The joints are connected by lightweight links. The active joint is driven by a dc motor through a harmonic drive gear reduction unit. The sweep of the active joint is limited to approximately 210 deg. The gear reduction harmonic drives provide speed reduction of 64:1 for the active joint. The dc motor is driven by a servo amplifier and is provided with an optical encoder and an analog tachometer.

Position and velocity feedback are available at the active joint. Position feedback is provided by incremental optical encoders. The position measurement of the passive joint is taken at the joint shaft using an optical encoder with 1000 pulses per resolution. Velocity feedback is from a dc generator tachometer, which is driven from the motor shaft. The velocity signal of the passive joint is obtained by filtered differentiation of the joint position.

The system diagram of the experimental apparatus is shown in Fig. 7. The planar manipulator is controlled from the 32-bit 80486 microcomputer via one input/output circuit board (DT2811-PGH) interfaced directly into the backplane of the computer. Command signals to the robot are sent to the power amplifiers through a 12-bit D/A converter. The range of the D/A is ± 5.0 V, yielding 10-mV resolution. Position feedback from the digital encoder is accessed by the computer through a digital I/O card. The encoder counts are then produced by the software. Resolution of the position is then 0.006283 rad for the passive and active joint. Velocity feedback from the tachometers are connected into a 12-bit A/D. This gives joint velocity resolution of 0.0005411 rad/s for the active joint.

The control algorithm was implemented on a microcomputer (PC 80486) and the signal processing in the experiments were carried out

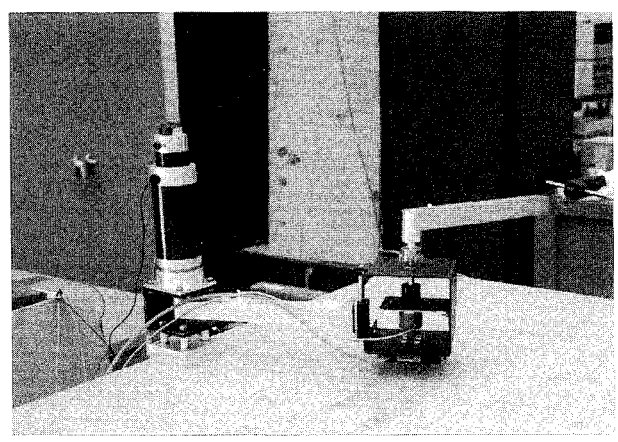

Fig. 6 Two-link planar passive-jointed experimental robot.

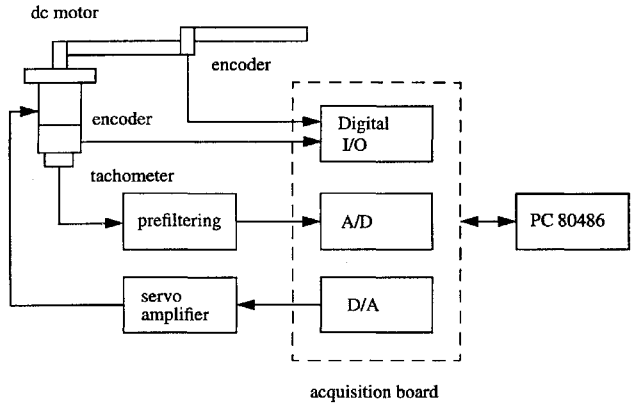

Fig. 7 System diagram of the experimental apparatus.

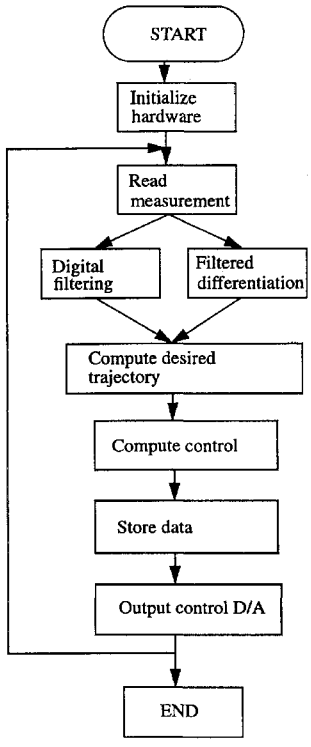

Fig. 8 Flowchart for the control program.

with a sampling rate of 2.9 kHz. The control program is written in the C programming language. The flowchart of the control program is given in Fig. 8.

B. Step Response Evaluation

The sliding mode controller was tested with a 60-deg step response shown in Fig. 9. The phase portrait of the step response is plotted in Fig. 10. By examining the system motion trajectory on a phase plane, we can intuit the basic aspects of the sliding mode control. As shown in Fig. 10, starting from initial condition $[0 \;\; 0]^T$, the trajectory is attracted to the boundary layer in 0.42 s and then slides toward the desired states $[\pi/3 \;\; 0]^T$.

C. Tracking Evaluation

The desired trajectory is $q_d = -(\pi/4)(1 - \cos \pi t)$. The maximum joint position displacement is $\pi/2$ rad and the maximum link angular velocity is $\pi^2/4$ rad/s. The result shown in Figs. 11 and 12 presents the passive joint tracking of the robot under sliding mode control. The computed torque controller tracking performance is shown in Figs. 13 and 14. The computed torque control shows larger tracking error when compared to the system performance under sliding mode control. The experimental performance of the passive jointed robot with sliding mode control is compared with the manipulator's performance when the computed torque control is used. Comparing the results in Figs. 13 and 14, it is concluded

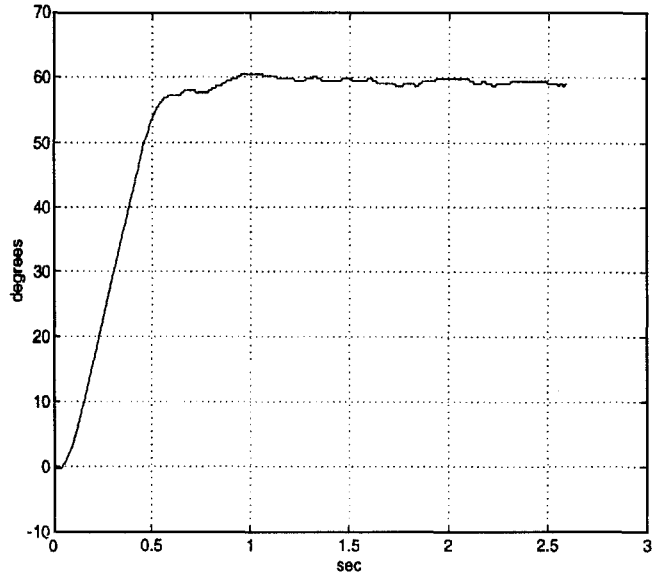

Fig. 9 Step response under sliding mode control.

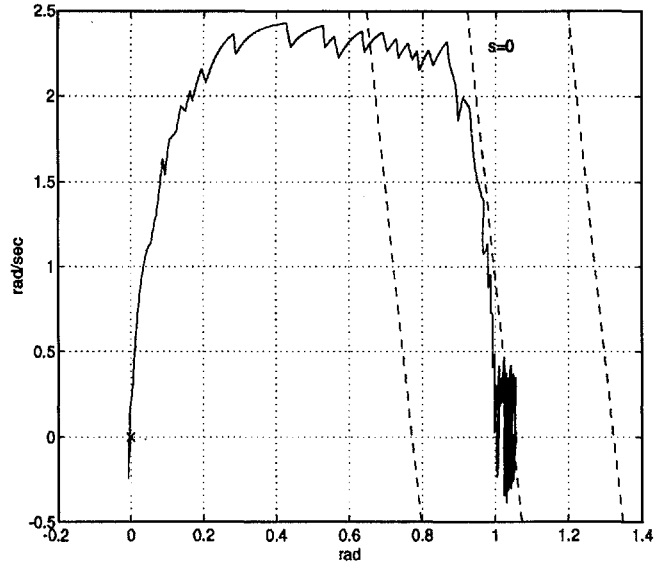

Fig. 10 Phase portrait of the step response.

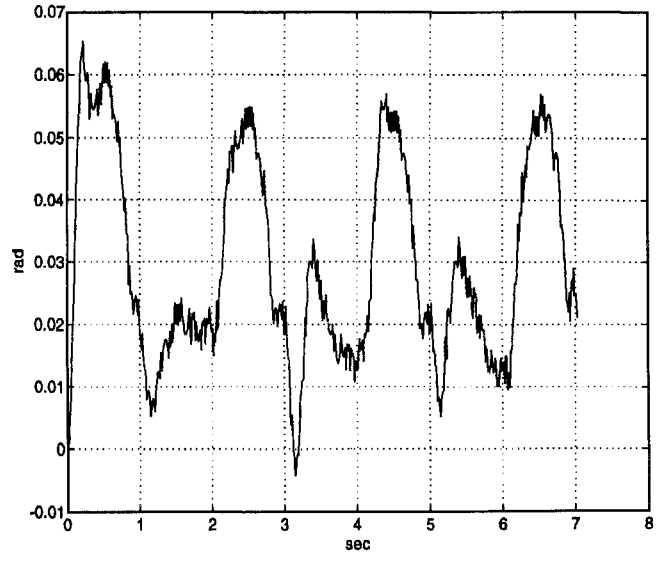

Fig. 11 Tracking error under sliding mode control.

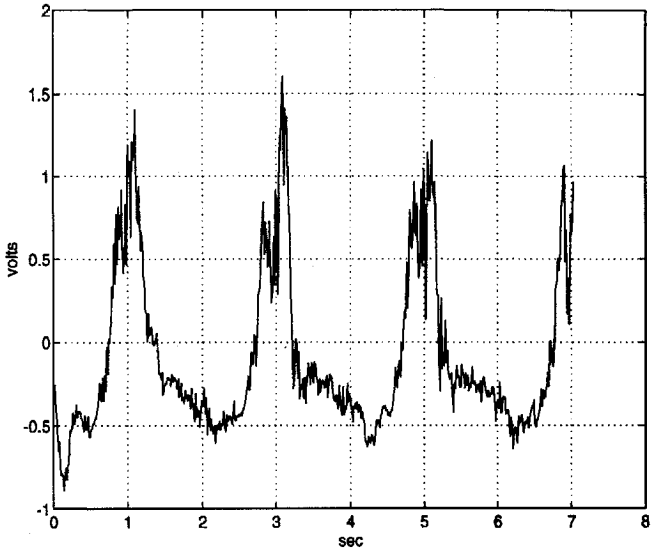

Fig. 12 Control signal under sliding mode control.

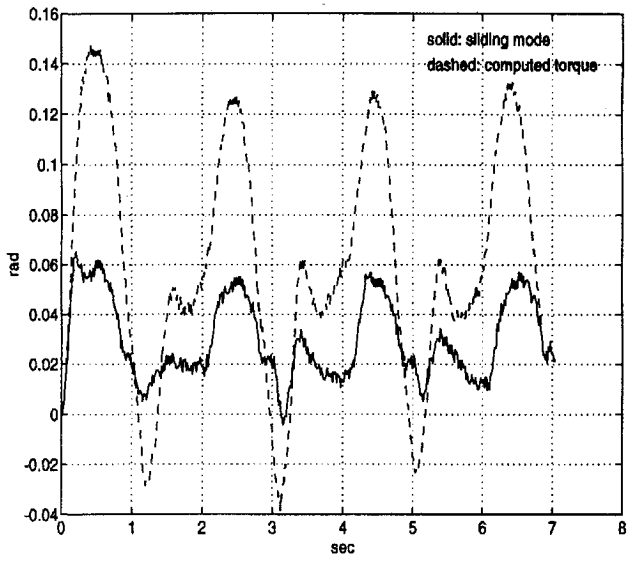

Fig. 13 Tracking error comparison.

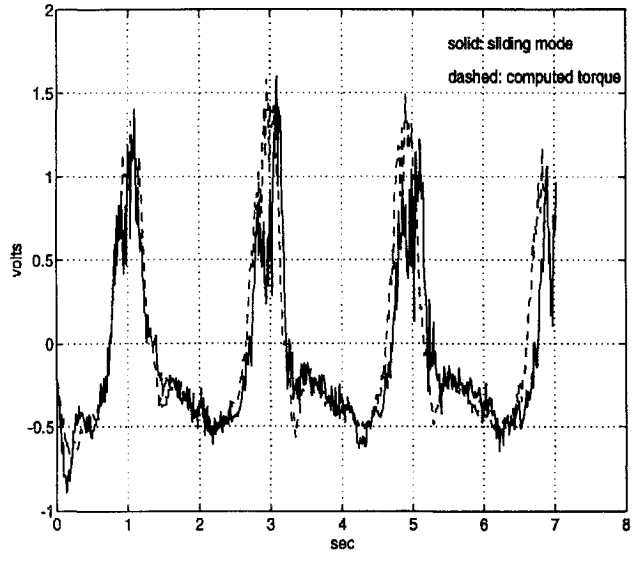

Fig. 14 Control signal comparison.

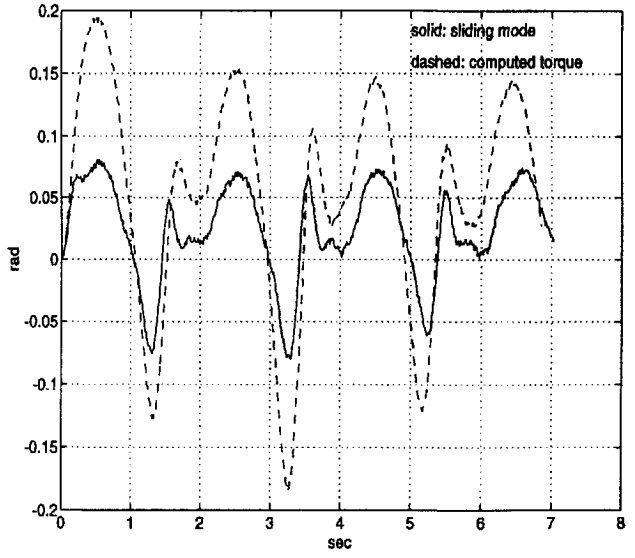

Fig. 15 Tracking error with increased payload.

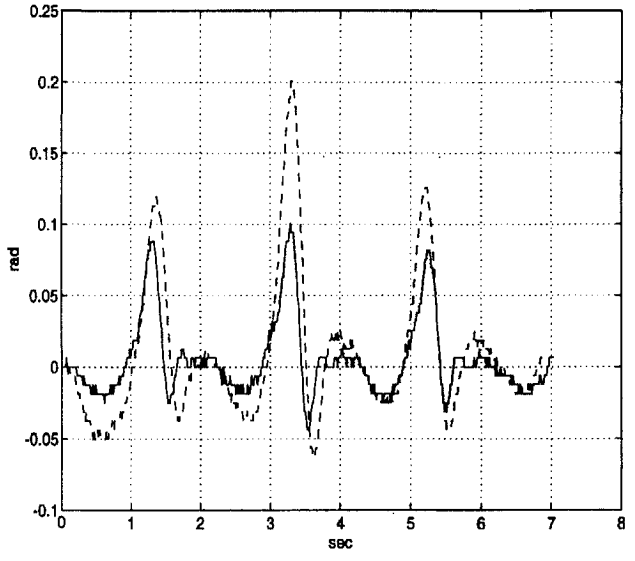

Fig. 16 Error change with increased payload.

that the robot under sliding mode control exhibits a smaller tracking error (50% less) when compared with the computed torque control.

D. Robustness Evaluation

An experiment was conducted to demonstrate the robustness to uncertainty in payload. The controller was designed for the nominal payload; but the payload of the arm was increased by 108% on the mass of the second link. The results given in Fig. 15 present the tracking performance under sliding mode control with increased payload. The error change with uncertainty in the payload is shown in Fig. 16. The sliding mode control performance shows smaller error change (20% less) when compared with the system behavior under computed torque control. The results clearly show the robustness of the sliding mode control in the presence of uncertainty in the dynamic model.

VI. Conclusions

This paper demonstrates the feasibility of the passive jointed robot. Coupling dynamics is utilized to control the angle of passive joints indirectly by controlling the active joints. A sliding mode control is designed and implemented on a microcomputer for a two-link passive-jointed robot. The robot is actuated by a dc motor and operated in the horizontal plane. It is assumed that dynamics of the robot is not exactly known. Based on variable structure system theory, a

control scheme is designed for trajectory tracking of the passive joint. The robustness of the sliding mode control is evaluated in presence of unknown payloads.

From numerical simulation results, the sliding mode scheme shows smaller tracking error when compared with the system performance under computed torque control. The performance of the sliding mode controller is validated by experiments. Experimental results show that the sliding mode scheme is superior to the computed torque method in terms of the passive joint tracking performance and robustness.

The control scheme studied can also be applied to the space manipulator system as a failure recovery controller. It is possible that the actuator of one joint of a manipulator system fails, but its brake and encoder still operate. Using the proposed control scheme, the failed joint can be driven into a desired position and then locked by using the brake. This application may be effective because it is important for a space robotic system to be able to tolerate a component or subsystem failure.

References

[1]Arai, H., and Tachi, S., "Position Control of a Manipulator with Passive Joints Using Dynamic Coupling," *IEEE Transactions on Robotics and Automation*, Vol. 7, No. 4, 1991, pp. 528–534.

[2]Papadopoulos, E., and Dubowsky, S., "Failure Recovery Control for Space Robotic Systems," *Proceedings of the American Control Conference* (Chicago, IL), Inst. of Electrical and Electronics Engineers, 1992, pp. 1485–1490.

[3]Mukherjee, R., and Chen, D., "Control of Free-Flying Underactuated Space Manipulators to Equilibrium Manifolds," *IEEE Transactions on Robotics and Automation*, Vol. 9, No. 5, 1993, pp. 561–570.

[4]Drazenovic, B., "The Invariance Conditions in Variable Structure Systems," *Automatica*, Vol. 5, No. 3, 1969, pp. 287–295.

[5]Young, K. D., "Controller Design for a Manipulator Using Theory of Variable Structure Systems," *IEEE Transactions on Systems, Man and Cybernetics*, Vol. 8, No. 2, 1978, pp. 101–109.

[6]Utkin, V. I., "Variable Structure Systems with Sliding Mode: A Survey," *IEEE Transactions on Automatic Control*, Vol. 22, No. 2, 1977, pp. 212–222.

[7]Itkis, U., *Control System of Variable Structure*, Wiley, New York, 1976, pp. 21–42.

[8]Drakunov, S. V., and Utkin, V. I., "Sliding Mode Control in Dynamic Systems," *International Journal of Control*, Vol. 55, No. 4, 1992, pp. 1029–1037.

[9]Paden, B. E., and Sastry, S. S., "Calculus for Computing Fillippov's Differential Inclusion with Application to the Variable Structure Control of Robot Manipulator," *IEEE Transactions on Circuits and Systems*, Vol. 34, No. 1, 1987, pp. 73–82.

[10]Slotine, J. J. E., and Sastry, S. S., "Tracking Control of Nonlinear Systems Using Sliding Surfaces with Applications to Robot Manipulators," *International Journal of Control*, Vol. 38, No. 2, 1983, pp. 465–492.

[11]Slotine, J. J. E., "Sliding Controller Design for Nonlinear Systems," *International Journal of Control*, Vol. 40, No. 2, 1984, pp. 465–492.

[12]Slotine, J. J. E., "The Robust Control of Robot Manipulators," *International Journal of Robotics Research*, Vol. 4, No. 2, 1985, pp. 49–63.

[13]Slotine, J. J. E., and Li, W., *Applied Nonlinear Control*, Prentice–Hall, Englewood Cliffs, NJ, 1991.

[14]Asada, H., and Slotine, J. J. E., *Robot Analysis and Control*, Wiley, New York, 1986, pp. 93–131.

[15]Asada, H., and Youcef-Toumi, K., *Direct-Drive Robots: Theory and Practice*, MIT Press, Cambridge, MA, 1987, pp. 45–122.

[16]Abdallah, C., Dawson, D., Dorato, P., and Jamshidi, M., "Survey of Robust Control for Rigid Robots," *IEEE Control Systems Magazine*, Vol. 11, No. 2, 1991, pp. 24–30.